



Single-cell transcriptomic analysis reveals the commonality of immune response upon H1N1 influenza virus infection in mice and humans

Yu Chen^{1,2†}, Huaiyuan Cai^{1,3†}, Qian Zhang^{1,4}, Gang Cao⁵, Jiahao Zhang^{1,3}, Bing Yang^{1,3*} and Jinxia Dai^{1,3*} 

Abstract

Seasonal influenza A virus (IAV), particularly the H1N1 subtype, poses a significant public health threat because of its substantial morbidity and mortality rates worldwide. Understanding the immune response to H1N1 is crucial for developing effective treatments and vaccines. In this study, we deciphered the single-cell transcriptomic landscape of peripheral blood mononuclear cells (PBMCs) from H1N1-infected humans and lung tissue samples from H1N1-infected mice by mining H1N1-related single-cell RNA sequencing data from the GEO database. We observed similar changes in immune cell composition following H1N1 infection, with an increase in macrophages but a decrease in T cells in both species. Moreover, significant transcriptional changes in bystander immune cells upon H1N1 infection were identified, with the upregulation of the chemokine *CCL2* in human PBMCs and increased expression of interferon-stimulated genes such as *Ifit3*, *Ifit1* and *Isg15* in mouse pulmonary immune cells. Intercellular cross-talk analysis highlighted enhanced interactions among bystander immune cells during H1N1 infection, with neutrophils in humans and macrophages in mice showing the most remarkable increases in interaction intensity. Transcription factor analysis revealed the conserved upregulation of key antiviral regulons, including STAT1 and IRF7, in T cells across both species, highlighting their pivotal roles in antiviral defense. These results suggest that humans and mice exhibit common immune responses to H1N1 infection, underscoring the similarity of vital immune mechanisms across species. The conserved immune mechanisms identified in this study provide potential therapeutic targets for enhancing antiviral immunity. Our research underscores the importance of understanding species-specific and conserved immune responses to H1N1 and offers insights that could inform the development of novel antiviral therapies and improve clinical outcomes for individuals affected by influenza.

Keywords Influenza A virus, H1N1, Single-cell transcriptomic analysis, Immune response, Bystander immune cells, Peripheral blood mononuclear cells

Communicated by Zhong Peng.

[†]Yu Chen and Huaiyuan Cai contributed equally to this work and share first authorship.

*Correspondence:

Bing Yang
yangbing@mail.hzau.edu.cn
Jinxia Dai
jxdai@mail.hzau.edu.cn

Full list of author information is available at the end of the article

Introduction

Seasonal influenza A virus (IAV) infection results in significant morbidity and mortality worldwide and is a major public health concern (Li et al. 2024; Yang et al. 2022). Seasonal IAV mainly includes the H1N1 and H3N2 subtypes, of which the H1N1 subtype is one of the most devastating IAVs, affecting millions annually with varying severity across different populations (Gostic et al.



© The Author(s) 2024. **Open Access** This article is licensed under a Creative Commons Attribution 4.0 International License, which permits use, sharing, adaptation, distribution and reproduction in any medium or format, as long as you give appropriate credit to the original author(s) and the source, provide a link to the Creative Commons licence, and indicate if changes were made. The images or other third party material in this article are included in the article's Creative Commons licence, unless indicated otherwise in a credit line to the material. If material is not included in the article's Creative Commons licence and your intended use is not permitted by statutory regulation or exceeds the permitted use, you will need to obtain permission directly from the copyright holder. To view a copy of this licence, visit <http://creativecommons.org/licenses/by/4.0/>. The Creative Commons Public Domain Dedication waiver (<http://creativecommons.org/publicdomain/zero/1.0/>) applies to the data made available in this article, unless otherwise stated in a credit line to the data.

2019; Mao et al. 2020). According to data from the World Health Organization (WHO), there are approximately 1 billion cases of influenza globally each year, resulting in 290,000 to 650,000 respiratory deaths, with a significant burden on healthcare systems during peak seasons. The epidemic of H1N1 is more severe during the 2022/2023 winter season. Therefore, systematically exploring the pathogenicity and immune response of human populations infected with H1N1 is urgently needed.

The human immune system mounts a complex and multifaceted response to IAV infection, involving both the innate and adaptive immune responses (Iwasaki & Pillai 2014). Understanding these immune responses is crucial for developing effective vaccines and treatments (Krammer & Palese 2015). The innate immune response is the first line of defense against IAV infection and involves the activation of various immune cell types, which recognize viral components through pattern recognition receptors and subsequently produce cytokines and chemokines that orchestrate the antiviral response (Hage et al. 2022). Type I interferons, in particular, play a critical role in limiting viral replication and spread by inducing the expression of interferon-stimulated genes (ISGs) (Hage et al. 2022). However, the virus has evolved multiple strategies to evade or suppress these innate immune responses, contributing to its pathogenicity (Kasuga et al. 2021; White et al. 2021).

Single-cell sequencing technologies, such as single-cell RNA sequencing (scRNA-seq), have revolutionized our understanding of the immune response to virus infection (Sun et al. 2020; Wilk et al. 2020). These technologies allow for high-resolution analysis of gene expression profiles at the individual cell level, providing insights into the heterogeneity and dynamics of immune cell populations during infection. By applying scRNA-seq to samples from infected individuals, researchers have identified distinct subsets of immune cells, characterized their functional states, and revealed novel intercellular interactions that contribute to the immune response (O'Neill et al. 2021; Steuermaier et al. 2018; Wilk et al. 2020; Zhu et al. 2024). Recent studies have demonstrated that heterogeneity in innate immune induction could affect the entire course of IAV infection (Medaglia et al. 2022). Since IAV induces a complex immune response involving multiple cell types and signaling pathways, comparing the viral load in different cells, the immune response, and intercellular communication within distinct cell types is essential.

Here, we downloaded seven scRNA-seq datasets comprising PBMCs from H1N1-infected and uninfected human subjects and lung tissue samples from H1N1-infected and uninfected mice. Our comparative analysis revealed marked alterations in immune cell proportions, with increases in macrophages and decreases in T cells

postinfection in both species. Enhanced intercellular cross-talk and upregulation of critical regulons were observed, highlighting conserved mechanisms in antiviral responses. These findings provide crucial insights into influenza immunology, informing the development of more effective vaccines and therapeutics by identifying universal targets for enhancing antiviral immunity.

Results

Consistent changes in the proportions of macrophages and T cells between human PBMCs and mouse lungs upon H1N1 infection

To compare the immune response divergence to H1N1 infection in different species, we retrieved scRNA-seq data related to H1N1 infection from the GEO database. The dataset included peripheral blood mononuclear cells (PBMCs) from two H1N1-infected individuals (IAs) and two healthy controls (HCs), as well as immune cells from the lung tissues of two H1N1-infected mice (mIAs) and one healthy control mouse (mHC). During IAV infection, PBMCs can migrate to sites of infection, such as the respiratory tract, which is critical for mounting an effective immune response (Music et al. 2016; Vangeti et al. 2023).

After rigorous quality filtering and batch correction (Fig. S1A and B), the cell types were annotated on the basis of several marker genes. We identified T cells, B cells, neutrophils, monocytes, macrophages, dendritic cells, and basophils in human PBMCs and mouse lungs (Fig. 1A-D). The bubble plot of gene expression for cell type markers (Fig. 1E and F) and the expression heatmap of the top five genes of each cell type (Fig. S1C and D) confirmed the accuracy of our annotation.

Further analysis revealed changes in the composition of immune cells during H1N1 infection (Fig. 1G and H). Specifically, in the PBMCs of H1N1-infected humans, the proportions of neutrophils and macrophages increased after infection. Moreover, the percentage of T cells decreased (Fig. 1I). In mouse lungs, the proportions of macrophages and dendritic cells increased under H1N1 infection, with a concomitant decrease in T cells (Fig. 1J). The increased number of macrophages but decreased number of T cells in both species indicate that humans and mice exhibit similar immune response characteristics in terms of critical immune cell type composition upon H1N1 infection.

Similar immune response of bystander cells in human PBMCs and mouse lungs to H1N1 infection

In PBMCs from H1N1-infected humans, no RNA counts of influenza virus were detected. Thus, all the PBMCs of H1N1-infected humans were designated bystander cells (Fig. 1K). Conversely, in the lung tissues of H1N1-infected mice, H1N1 primarily infected some phagocytes, such as

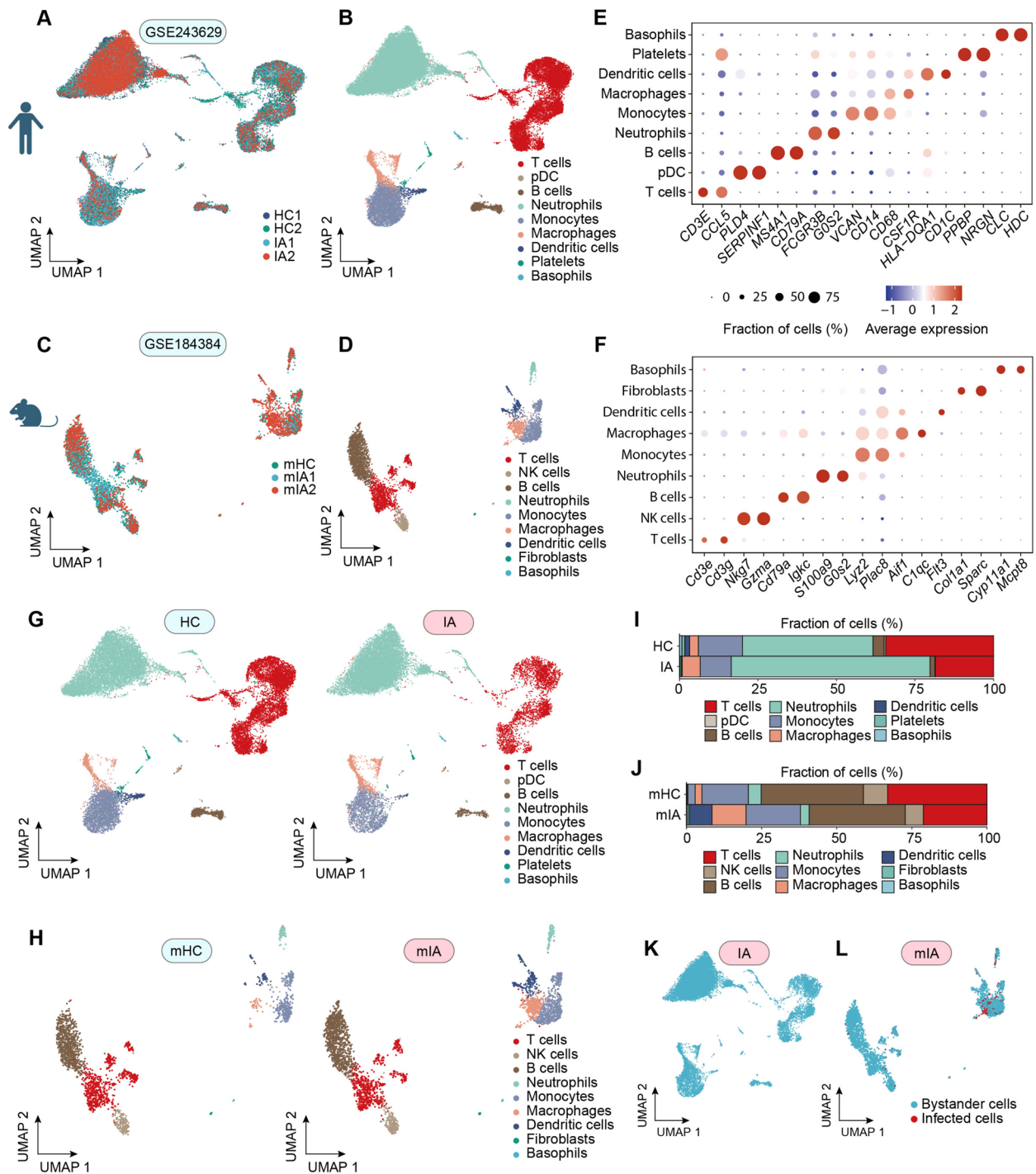


Fig. 1 Single-cell transcriptomic landscape of human PBMCs and mouse lung tissues infected with HIN1. **A** UMAP plot of human peripheral blood mononuclear cells (PBMCs) from the four samples indicated with different colors. HC: Human healthy control, IA: Human IAV infection, Gene Expression Omnibus (GEO): GSE243629. **B** UMAP plot of human PBMC cell clusters. **C** UMAP plot of mouse lung immune cells from three distinct samples. mHC: Mouse healthy control; mIA: Mouse IAV infection; GEO: GSE184384. **D** UMAP plot of mouse lung immune cell clusters. **E** Bubble plot of marker genes for different cell types in human PBMCs. **F** Bubble plot of marker genes for different immune cell types in mouse lungs. **G** UMAP of human PBMC clusters in the HC and IA groups. **H** UMAP of mouse lung immune cell clusters in the mHC and mIA groups. **I** Stacked bar plot for the proportions of different cell types in human PBMCs from the HA and IA groups. **J** Stacked bar plot for the proportions of different immune cell types in mouse lung tissues from the mHC and mIA groups. **K** UMAP of bystander cells in PBMCs from IAV-infected humans. **L** UMAP of bystander cells in lung tissues from IAV-infected mice. pDCs, plasmacytoid dendritic cells

macrophages, neutrophils and monocytes (Fig. S1E). We detected different expression patterns of H1N1 genes by comparing the expression levels of eight H1N1 gene segments in these infected lung tissue cells (Fig. S1F). Specifically, the *NS* gene presented the highest expression in macrophages, whereas the *PB2* gene was predominantly expressed in neutrophils (Fig. S1F).

Additionally, among the eight gene segments, only the *NP* gene presented relatively high expression in T cells (Fig. S1F). Similarly, uninfected cells in mouse lung tissues were defined as bystander cells (Fig. 1L). Bystander immune cells, although not directly infected by the virus, play a critical role in regulating or supporting the overall antiviral immune response and controlling infection. These cells utilize complex signaling and intercellular interactions to help establish an effective immune defense against viral infections (Iwasaki & Pillai 2014). To better understand the reactions of bystander immune cells to H1N1 infection across different species, we identified the transcriptomic signatures of these cells in various samples.

First, the differentially expressed genes (DEGs) of bystander immune cells in the H1N1-infected group, compared with those in the normal group, were identified across humans and mice (Table S1). The results revealed that the number of DEGs in B, dendritic, and T cells was relatively similar between humans and mice. However, the number of DEGs in mouse macrophages was greater than that in human macrophages. In addition, we found that the number of DEGs in human monocytes and neutrophils was greater than that in mouse monocytes and neutrophils (Fig. S2A). The consistency analysis of DEGs among different types of immune cells between humans and mice revealed that the number of homologous DEGs across immune cell types ranged from 91–280 (Fig. S2B, Table S1).

In the volcano plots of the DEGs, the top 3 upregulated and downregulated genes are highlighted (Fig. 2A and B). Under H1N1 infection, significant upregulation of *CCL2* was observed in T cells, B cells, dendritic cells, macrophages, and neutrophils in human PBMCs (Fig. 2A). As a crucial chemokine, the elevated transcriptional level of *CCL2* prompted the active mobilization of immune

cells toward the infection site, reflecting the widespread immune activation induced by H1N1 infection. In contrast, in multiple bystander immune cells in mouse lung tissue, interferon-stimulated genes, such as *Ifit3*, *Ifit1* and *Isg15*, were significantly upregulated (Fig. 2B). These genes are activated under intense interferon stimulation, suggesting that bystander immune cells in the pulmonary microenvironment are influenced by interferons, thereby increasing their antiviral capabilities and reinforcing the overall antiviral immune response.

Considering the high proportion of T cells in immune cells and the consistent proportion change in T cells upon H1N1 infection between humans and mice (Fig. 1I and J), we focused on T cells for the following analysis. To explore pathway changes induced by H1N1 infection, we performed KEGG and GOBP enrichment analyses on DEGs in bystander T cells. KEGG pathway enrichment revealed that H1N1 infection drove similar immune responses and signaling pathway activation in bystander T cells across both species, including the influenza A, hepatitis C, and measles pathways. Antigen processing and presentation pathways were also enriched, highlighting the role of bystander T cells in recognizing and eliminating virus-infected cells (Fig. 2C and D). GOBP analysis revealed significant enrichment in biological processes such as the response to viruses and the defense response to viruses, indicating that bystander T cells initiate and regulate antiviral defense mechanisms (Fig. 2E and F). Overall, these analyses revealed that H1N1 infection triggered complex immune signaling networks in bystander T cells and revealed the essential role of bystander T cells in effective antiviral defense.

Following H1N1 infection, bystander T cells from both humans and mice presented significant upregulation of several essential genes involved in antiviral responses, including human *MX1*, *MX2*, *STAT1*, *ISG20*, *IRF7*, *RSAD2*, *IFIH1*, *CXCL10*, *IFI30*, and their homologs in mice (Fig. 2G and H, Fig. S2C and D). The consistent changes in the expression of these genes underscored the conserved nature of immune responses to H1N1 infection across species. *MX1* and *MX2* are interferon-induced GTPases known for their potent antiviral activities against RNA viruses (Wang et al. 2020). The

(See figure on next page.)

Fig. 2 Differentially expressed genes (DEGs) of bystander immune cells in H1N1-infected samples from humans and mice. **A** Volcano plot of DEGs in bystander immune cells from H1N1-infected individuals. **B** Volcano plot of DEGs in bystander immune cells from H1N1-infected mice. **C** Circle plot for KEGG enrichment analysis of DEGs in bystander T cells from humans. **D** Circle plot for KEGG enrichment analysis of DEGs in bystander T cells from mice. **E** Bubble plot of the results of the GOBP enrichment analysis of DEGs in bystander T cells from humans. **F** Bubble plot of the results of the GOBP enrichment analysis of DEGs in bystander T cells from mice. **G** Violin plots of the differential expression of antiviral response-related genes in bystander T cells from H1N1-infected and uninfected individuals. **H** Violin plots of the differential expression of antiviral response-related genes in bystander T cells from H1N1-infected and uninfected mice. HC: Human healthy control, IA: Human IAV infection, mHC: Mouse healthy control, mIA: Mouse IAV infection

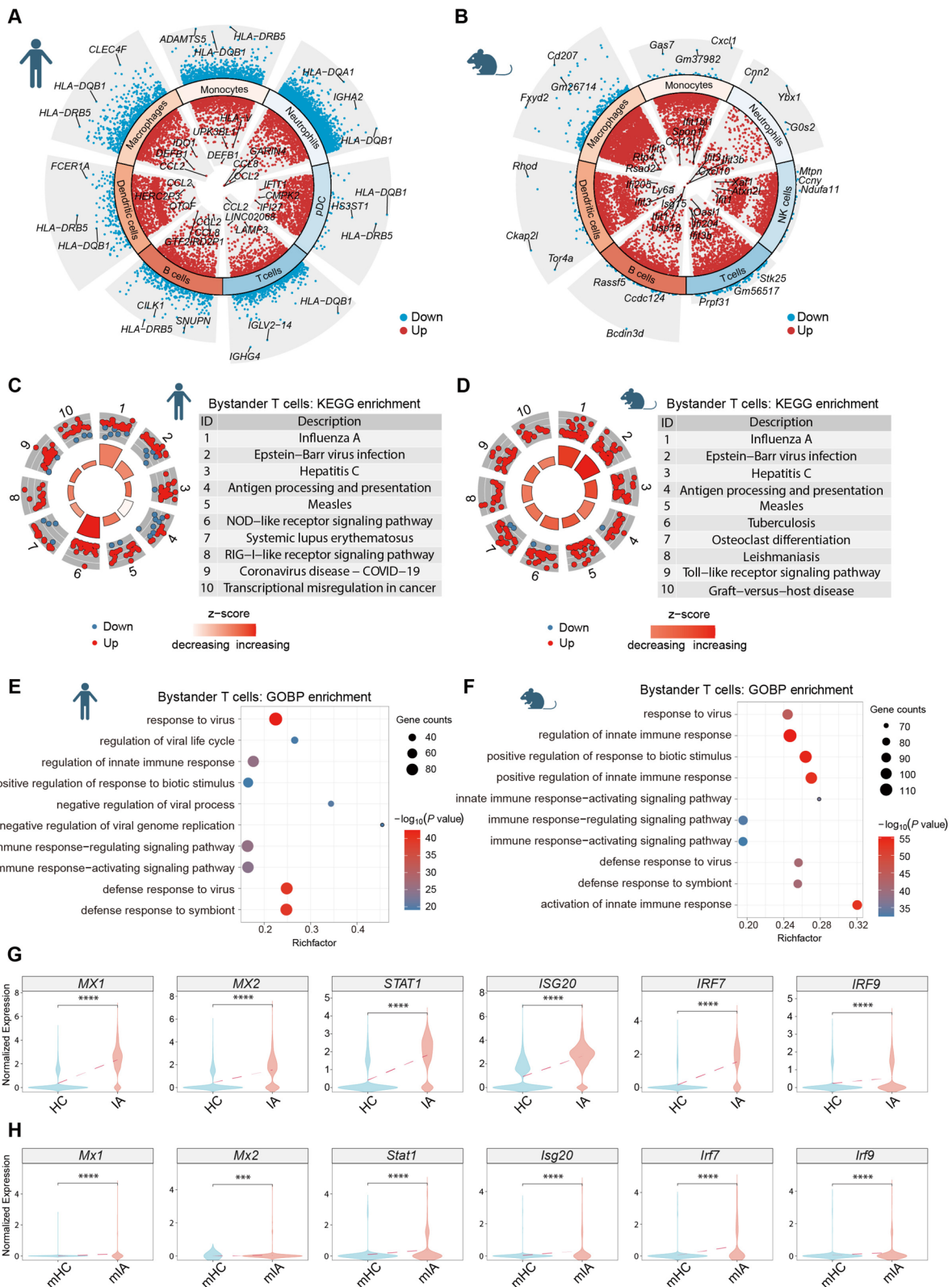


Fig. 2 (See legend on previous page.)

upregulation of these genes suggests an increased ability of bystander T cells in humans and mice to inhibit viral replication upon H1N1 infection. The increased expression of *STAT1*, a critical transcription factor in the interferon signaling pathway, may further support the antiviral response of bystander T cells. *STAT1* mediates the transcription of downstream antiviral effectors, including *MX1* and *MX2*, thereby reinforcing antiviral defense mechanisms in bystander T cells (Kim et al. 2016). The upregulation of *ISG20* in both species underscores its role as an interferon-stimulated gene with RNase activity, contributing to the degradation of viral RNA and restricting viral replication. The coordinated increase in *IRF7* and *IRF9* expression further enhances the antiviral response by amplifying interferon production and regulating downstream immune signaling pathways (Lazear et al. 2019). The increased expression of these antiviral genes collectively indicated that bystander T cells from both humans and mice could activate a robust and conserved antiviral program following H1N1 infection. The shared upregulation of *MX1*, *MX2*, *STAT1*, *ISG20*, *IRF7*, and *IRF9* homologous genes in both mice and humans highlights the similarities in how bystander T cells respond to and combat H1N1 infection. Further exploration into the specific roles of these genes in bystander T cell-mediated immunity against IAV infection will be crucial for effectively advancing strategies to combat influenza infections.

Enhanced cross-talk among specific bystander immune cells in human PBMCs and mouse lungs upon H1N1 infection

In the context of IAV infection, cross-talk between various bystander immune cells plays a pivotal role in shaping the immune response. In our research, CellChat analysis of bystander immune cells revealed intricate interactions among multiple cell populations in both mice and humans. In both humans and mice, the number and strength of interactions among bystander immune cells increased upon H1N1 infection (Fig. 3A and B). To identify which intercellular interactions were most

altered and contributed to the overall increase in intercellular cross-talk, we generated heatmaps illustrating the interactions among various bystander immune cells. In human PBMCs, the most notable increase in the number of interactions with H1N1 infection was observed between T cells and macrophages (Fig. 3C). Macrophages displayed increased interactions with most cell types, except for neutrophils (Fig. 3C). Monocytes also showed increased interactions with most cell types, except for a reduction in interactions with B cells (Fig. 3C). The interaction intensity among neutrophils markedly increased following H1N1 infection, suggesting that the increased interactions among bystander immune cells in human PBMCs after H1N1 infection are likely mediated primarily by neutrophils (Fig. 3C). In mouse lung tissues, macrophages exhibited increased internal interaction numbers and strengths following H1N1 infection (Fig. 3D). Additionally, the intensity of interactions between macrophages as senders and other bystander immune cells also increased to some extent (Fig. 3D).

The analysis of overall signaling patterns revealed several pathways conserved between humans and mice, including the CCL and TGF- β pathways (Fig. 3E and F). In control human PBMCs, the CCL signaling pathway was predominantly active in T cells (Fig. 3E). Under H1N1 infection, in addition to T cells, the CCL signaling pathway was enhanced in neutrophils (Fig. 3E). Moreover, there was a marked increase in CCL pathway interactions between T cells and neutrophils, as well as between T cells and monocytes (Fig. 3G). In control mice, the CCL signaling pathway was most active in monocytes (Fig. 3F), with monocytes serving as the primary receivers of CCL signals (Fig. 3H). Upon H1N1 infection, in addition to monocytes, neutrophils, macrophages, and dendritic cells also emerged as significant receivers of CCL signals, and the interactions among various bystander immune cells through the CCL signaling pathway became more complex (Fig. 3H). A detailed examination of the contributions of different ligand–receptor pairs in the CCL signaling pathway across various groups revealed that in humans, the *CCL5–CCR1* ligand–receptor pair played a

(See figure on next page.)

Fig. 3 Intercellular cross-talk of different bystander immune cells in humans and mice infected with H1N1. **A** Bar plot for the overall number of bystander immune cell interactions in H1N1-infected and uninfected humans and mice. **B** Bar plot for the overall strength of bystander immune cell interactions in H1N1-infected and uninfected humans and mice. **C** Heatmap of the differences in the number and strength of interactions between bystander immune cells in H1N1-infected and uninfected individuals. **D** Heatmap of the differences in the number and strength of interactions between bystander immune cells in H1N1-infected and uninfected mice. **E** Heatmap of the overall signaling patterns of bystander immune cells in H1N1-infected human samples compared with those in uninfected human samples. **F** Heatmap of the overall signaling patterns of bystander immune cells in H1N1-infected mouse samples compared with those in uninfected mouse samples. **G** Chord plot of the CCL pathway interactions between bystander immune cells in H1N1-infected and uninfected human samples. **H** Chord plot of the CCL pathway interactions between bystander immune cells in H1N1-infected and uninfected mouse samples. HC: Human healthy control, IA: Human IAV infection, mHC: Mouse healthy control, mIA: Mouse IAV infection

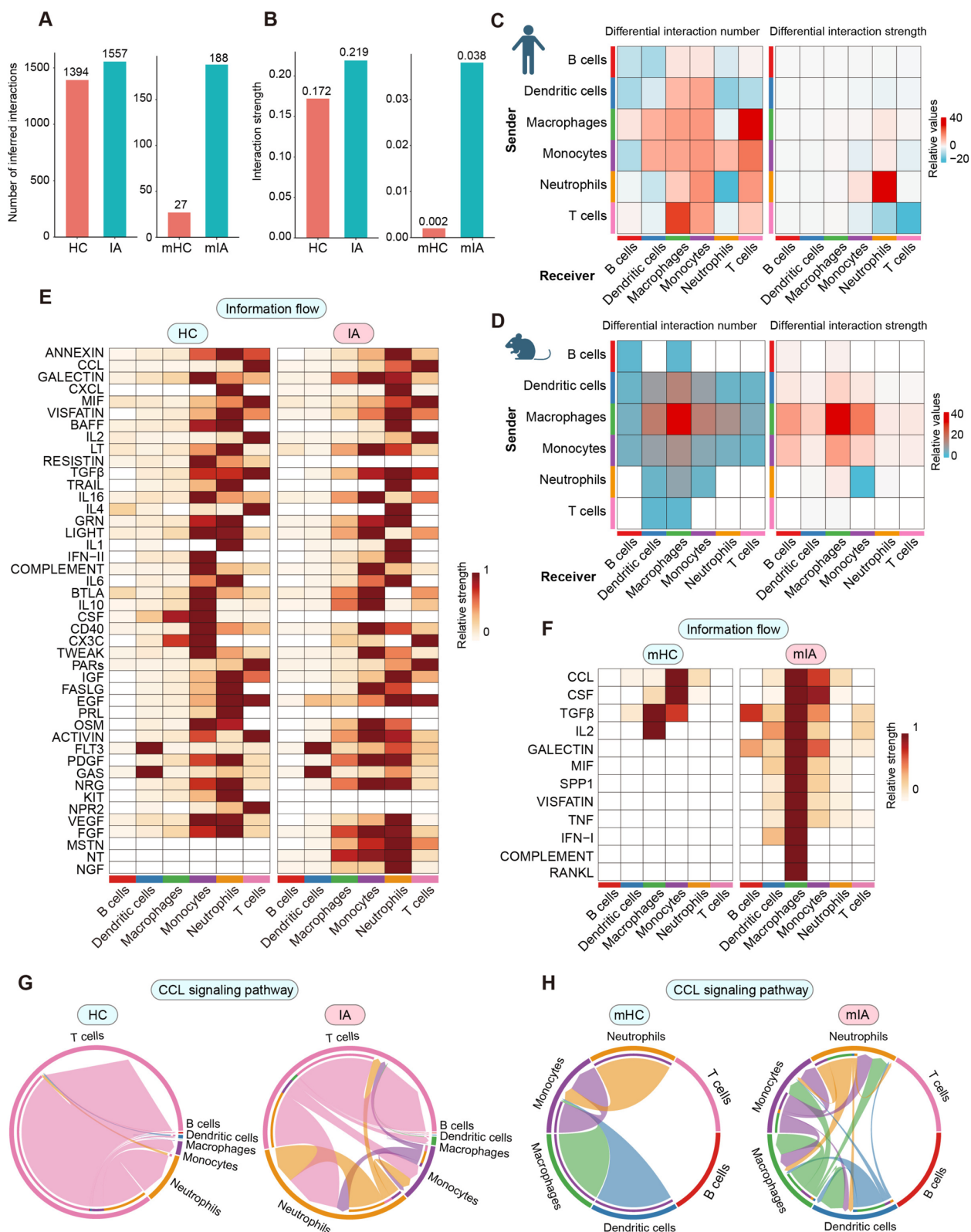


Fig. 3 (See legend on previous page.)

significant role in both control and H1N1 infection samples (Fig. S3A). In mice, the *Ccl6-Ccr2* ligand–receptor pair was predominant in the CCL pathway in both control and H1N1-infected samples (Fig. S3A). The interaction network of these ligand–receptor pairs indicated that in humans, the interaction between T cells and neutrophils via the *CCL5-CCR1* pair increased during H1N1 infection (Fig. S3B). In mice, macrophages and monocytes exhibited a notable increase in interactions through the *Ccl6-Ccr2* pair under H1N1 infection (Fig. S3B). In addition to the CCL pathway, the TGF- β pathway also plays a crucial role in influenza immunity (Zhao et al. 2024). It protects the host from immune-mediated damage by inhibiting excessive inflammation and promoting the function of regulatory T cells. Interestingly, we found that following H1N1 infection, T cells predominantly act as signal receivers in the TGF- β pathway for both species (Fig. S3C–E). In humans, the primary signal senders are neutrophils, whereas in mice, the primary signal senders are monocytes (Fig. S3C). In both humans and mice, the TGF- β pathway interactions were mediated by the *TGFB1-(TGFBRI+TGFBRII)* and *Tgfb1-(Tgfbri1+Tgfbri2)* ligand–receptor pairs, respectively (Fig. S3D). Under H1N1 infection, T cells of both species receive *TGFB1* signals by expressing *TGFBRI* and *TGFBRII* (*Tgfbri1* and *Tgfbri2* in mice) receptors (Fig. S3E).

Shared upregulation of certain regulons in bystander T cells across humans and mice

Understanding transcriptional regulation in bystander T cells will offer critical insights into the immune response mechanisms to H1N1 infection in different species. We thus analyzed differentially activated regulons in bystander T cells from H1N1-infected humans and mice compared with their normal controls. Several regulons, specifically IRF7(+) and members of the *STAT* family in humans, as well as their homologous genes in mice, were commonly upregulated in both species upon H1N1 infection (Fig. 4A and B). Under H1N1 infection, bystander T cells in human PBMCs and mouse lung tissues presented significantly increased activity of IRF7(+) and *Irf7*(+), *STAT1*(+) and *Stat1*(+), and *STAT2*(+) and *Stat2*(+) (Fig. 4C), indicating their crucial roles in the antiviral response.

The increased activity of IRF7(+) and *Irf7*(+), as well as that of *STAT1*(+) and *Stat1*(+), in bystander T cells from humans and mice following H1N1 infection underscores their essential roles in antiviral defense. IRF7 is a key transcription factor of type I interferon responses and is pivotal for activating interferon-stimulated genes (ISGs) that inhibit viral replication (Zhou et al. 2022). The concurrent upregulation of *STAT1*, a critical component of the interferon signaling pathway, further enhances the

antiviral response by driving the expression of additional ISGs (Ren et al. 2023).

Further analysis of the IRF7(+) and *Irf7*(+) regulation networks in humans and mice revealed numerous shared downstream target genes, such as *STAT1*, *STAT2*, *IRF7*, *JAK2*, *ISG15* and *ISG20*, in humans and homologous genes in mice, suggesting a conserved antiviral defense mechanism (Fig. 4D). These genes are integral to the interferon signaling cascade and play vital roles in enhancing the antiviral state of T cells (Bonjardim et al. 2009; Crouse et al. 2015). For example, *ISG15* and *ISG20* are involved in the degradation of viral RNA, whereas *JAK2* participates in the JAK-STAT signaling pathway, which mediates the response to interferons (Bohlen et al. 2023; Perng & Lenschow 2018; Stadler et al. 2021).

These findings provide significant insights into the transcriptional regulation of bystander T cells during H1N1 infection. The conserved enhancement of IRF7(+) and *Irf7*(+), as well as *STAT1*(+) and *Stat1*(+) activity across different species following H1N1 infection, underscores the importance of these regulons in the antiviral immune response. This conservation suggests potential therapeutic targets for enhancing antiviral immunity in humans by modulating the activity of these key transcription factors and their downstream pathways.

Overall, the similar activation of regulons in bystander T cells from H1N1-infected human and mouse samples highlights the complex transcriptional networks that underpin the immune response to viral infections. The integration of these results highlights how shared regulatory mechanisms across species can inform the development of novel therapeutic strategies to increase the immune response against H1N1 infections. Further investigation into these regulatory pathways will be crucial for developing effective interventions to enhance antiviral defenses and improve clinical outcomes in individuals affected by H1N1.

Discussion

scRNA-seq has revolutionized our understanding of complex biological processes by enabling gene expression analysis at the individual cell level. This technology has provided profound insights into various biological phenomena, including intercellular heterogeneity, developmental processes, and disease mechanisms, particularly viral infections (Park et al. 2020; Sun et al. 2020). Recent studies have demonstrated the power of scRNA-seq in exploring the pathogenesis of influenza virus (Boyd et al. 2020; Dai et al. 2023; O'Neill et al. 2021; Steuerman et al. 2018). For example, scRNA-seq has been used to profile host and viral transcripts simultaneously, providing a comprehensive view of the host's response to influenza virus infection and how the virus adapts to and

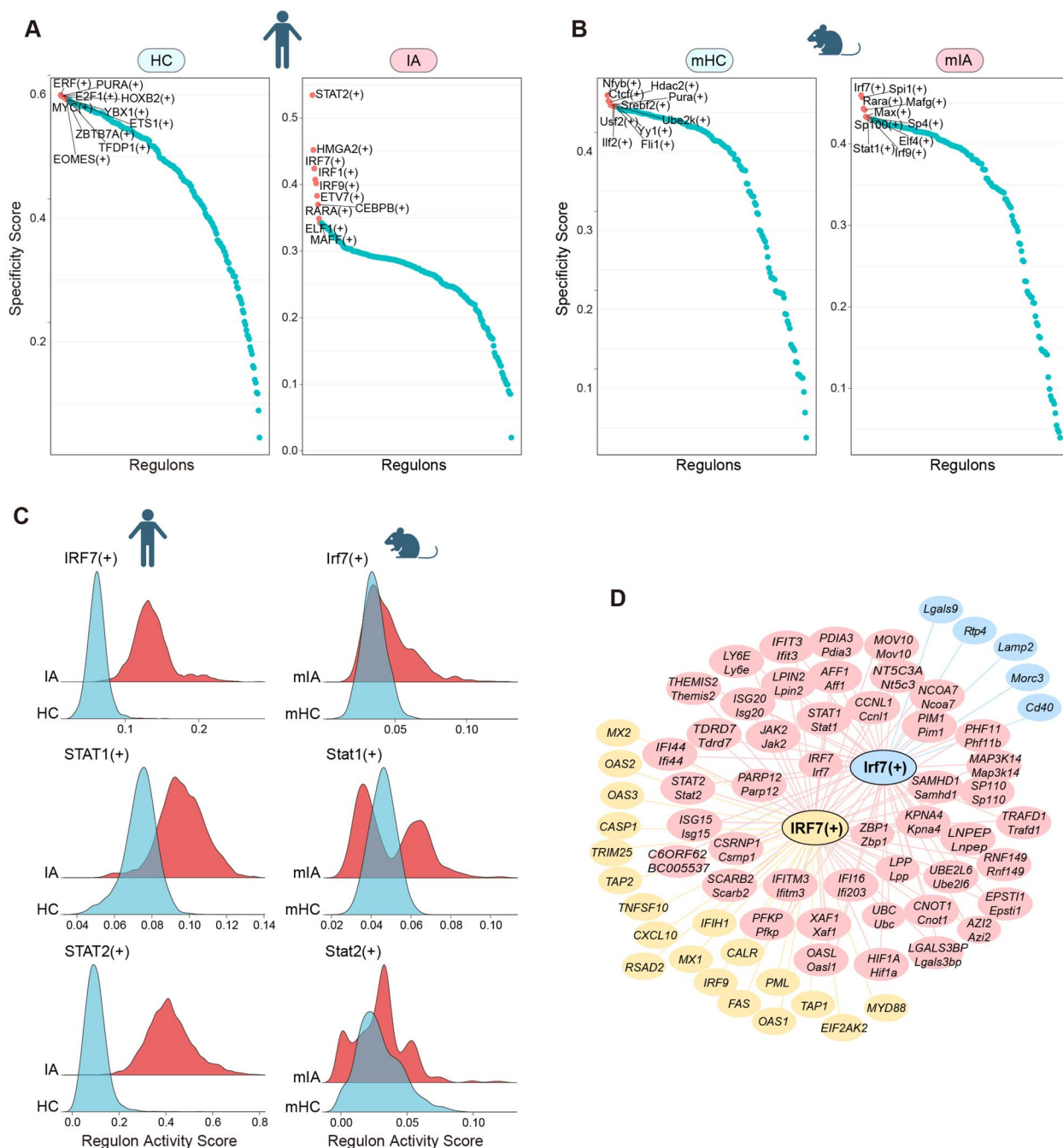


Fig. 4 Transcription factor regulation in bystander T cells from humans and mice infected with H1N1. **A** Scatter plot of regulon specificity scores for bystander T cells in H1N1-infected and uninfected human samples. **B** Scatter plot of regulon specificity scores for bystander T cells in H1N1-infected and uninfected mouse samples. **C** Ridge plot of the regulon activity scores for IRF7(+), STAT1(+), STAT2(+), Irf7(+), Stat1(+), and Stat2(+). **D** Regulatory network diagram of the IRF7(+) and Irf7(+) regulons, with pink indicating genes detected in both the IRF7(+) and Irf7(+) groups, yellow indicating genes detected only in the IRF7(+) group, and light blue indicating genes detected only in the Irf7(+) group. HC: Human healthy control, IA: Human IAV infection, mHC: Mouse healthy control, mIA: Mouse IAV infection

evolves within the host (O'Neill et al. 2021; Steerman et al. 2018). Here, we downloaded 7 scRNA-seq datasets comprising PBMCs from H1N1-infected and uninfected

human subjects and lung tissue samples from H1N1-infected and uninfected mice. Our study reveals several key findings regarding the response and interaction of

immune cells during H1N1 infection, emphasizing the crucial roles of bystander cells by profiling their immune characteristics, intercellular cross-talk, and transcription factor regulation.

We also found that the changes in immune cell populations following H1N1 infection differ between mice and humans, which may be attributed primarily to the distinct characteristics of the samples used (PBMCs from humans and lung tissues from mice). Additionally, species-specific adaptations may also contribute to these observed differences. Humans and mice have distinct immune system architectures, including differences in cytokine signaling, cell receptor expression, and transcription factor expression, which may explain the divergent immune responses. These interspecies differences highlight the challenges of directly translating findings from mouse models to humans. Despite these differences, the shared immune response patterns, particularly in T cells, support the conservation of core immune mechanisms. Further elucidation of the commonalities and differences in immune responses between humans and mice following H1N1 infection can provide deeper insights for personalized treatment of H1N1 infection in humans.

Our analysis indicated that both human PBMCs and mouse lung tissues exhibited similar shifts in immune cell composition following H1N1 infection. Notably, we detected an increased proportion of macrophages but a marked reduction in the T-cell proportion. These findings suggest fundamental similarities in the immune response mechanisms between these species. The increase in macrophages indicates their function in antigen presentation and cytokine production, which are essential for coordinating the adaptive immune response (Gordon & Pluddemann 2018). Interestingly, despite their expected accumulation at infection sites, the reduction in T-cell proportions suggests complex regulation of T-cell dynamics that might involve migration patterns or local tissue-specific signals. This phenomenon could be attributed to the apoptosis or migration of T cells to other tissues and the potential suppression of T-cell proliferation by viral infection (Pizzolla & Wakim 2019).

Bystander immune cells, which are not directly infected by the virus, play a critical role in supporting the overall antiviral response. Our study revealed that these cells, notably T, B, and dendritic cells, presented significant transcriptomic alterations upon H1N1 infection. The upregulation of the chemokine *CCL2* in human PBMCs and the expression of interferon-stimulated genes (ISGs), such as *Ifit3*, *Ifit1* and *Isg15*, in mouse lung tissues highlights the importance of these signaling molecules in mobilizing and activating bystander immune cells. Chemokines such as *CCL2* are crucial for recruiting

monocytes and other immune cells to the site of infection, thereby enhancing the immune response (Deshmane et al. 2009). Similarly, ISGs are vital in establishing an antiviral state within cells, limiting viral replication and spread (Schoggins & Rice 2011).

Successful virus control and elimination require concerted cooperation across diverse immune cell types. Our intercellular cross-talk analysis revealed a substantial increase in interaction numbers and strengths among bystander immune cells following H1N1 infection. In human PBMCs, neutrophils demonstrated the most notable increase in interaction strength, whereas macrophages showed increased interactions in mouse lung tissues. This adaptation may be due to the evolutionary strategies developed by different species to combat viral infections. The activation of the CCL signaling pathway in multiple cell types underscores the critical role of chemokine signaling in mediating these interactions (Russell et al. 2017). Enhanced cross-talk between immune cells facilitates a coordinated response, allowing different cell types to synergize in combating the virus. This intricate communication network is vital for practical immune function. Such dynamic intercellular communication is essential for mounting a swift and robust immune response, facilitating viral clearance, and limiting virus spread.

The identification of the conserved upregulation of crucial transcription factors, such as *STAT1* and *IRF7*, in bystander T cells from both humans and mice underscores their pivotal roles in antiviral immunity. These transcription factors are integral to the interferon signaling pathway, driving the expression of ISGs that inhibit viral replication. The shared upregulation of genes such as *MX1*, *MX2*, *STAT1*, *ISG20*, *IRF7* and *IRF9* in humans and their homologous genes in mice emphasized the conserved nature of the antiviral response across species. These findings suggest potential therapeutic targets for enhancing antiviral immunity by modulating the activity of these key transcription factors and their downstream pathways. For example, targeting the *STAT1* pathway could amplify the antiviral response, providing an approach to increase immunity against IAV (Ivashkiv & Donlin 2014; Schoggins 2014). Therefore, a better understanding of the conserved mechanisms of immune responses across species can help identify universal antiviral therapy targets. Targeted regulation of *STAT1* and *IRF7* enhances ISG activity and thus improves the capacity of bystander T cells.

Several studies have validated the critical roles of potential therapeutic targets in antiviral immune responses, particularly in the context of IAV infection. For example, Hemann et al. demonstrated that IFN- λ coordinates innate and adaptive immune responses by

regulating DC migration and the IL-10 immunoregulatory network, leading to effective antiviral T-cell immunity during IAV infection (Hemann et al. 2019). As the critical transcription factor in the interferon signaling pathway, Syk-induced STAT1 activation is critical for initial antiviral immunity during IAV infection (Liu et al. 2021). Mutations in IRF7 can hinder sufficient interferon generation, resulting in severe influenza infection (Ciancanelli et al. 2015). ISG15, an interferon-induced ubiquitin-like protein, inhibits a wide range of viruses, including IAV, by conjugating with target proteins (Zhao et al. 2013). These studies strongly support the feasibility of these potential therapeutic targets for anti-IAV infections. However, further functional confirmation experiments for these potential therapeutic targets need to be performed in the future.

Conclusion

In conclusion, our study highlights the commonality of immune responses to H1N1 infection in humans and mice, emphasizing the critical roles of bystander immune cells, intercellular cross-talk, and transcription factor regulation. These findings will support the development of novel therapeutic strategies to enhance antiviral defenses and improve clinical outcomes for individuals affected by H1N1. By leveraging the conserved mechanisms identified in this study, we can advance our understanding of viral immunology and lay the foundation for more effective treatments against influenza and other viral infections.

Methods

scRNA-seq data acquisition and quality control

The scRNA-seq data from humans and mice were downloaded from the GEO database with accession numbers GSE243629 (Zhang et al. 2023) and GSE184384 (Beppu et al. 2023), respectively. Human single-cell transcriptomic data were processed via CellScope (version 2.0.7) for alignment and quantification, with the reference genome and annotation files (GRCh38.p14) obtained from GENCODE (<https://www.genencodegenes.org/human/>, Release 45). Mouse single-cell transcriptomic data were processed via Cell Ranger (version 7.2.0) for alignment and quantification, with the reference genome and annotation files (GRCm39) obtained from GENCODE (<https://www.genencodegenes.org/mouse/>, Release M35). The H1N1 reference genome data were downloaded from NCBI via data from the PR8 strain. Subsequent dimensionality reduction and clustering analyses were conducted via the Seurat package (version 5.0.1) (Hao et al. 2024) in R (V. 4.3.2). Initially, genes expressed in fewer than three cells per sample were filtered out, and

low-quality cells were removed on the basis of gene count and mitochondrial contamination. The filtering criteria for human samples were as follows: genes with gene counts between 350 and 5000, UMI counts greater than 460, log10GenesPerUMI greater than 0.835, and mitochondrial gene content less than 20%. For mouse samples, the criteria were cells with gene counts between 70 and 6000, UMI counts greater than 80, log10Genes per UMI greater than 0.835, and a mitochondrial gene content less than 10%.

Dimensionality reduction and clustering analysis

After data filtering, human and mouse samples were processed. The data were normalized via the `normalizeData` function to convert raw counts to a comparable scale across cells. The `ScaleData` function was subsequently applied to center and scale the expression data for each gene to adjust for variability due to sequencing depth and technical noise, thus facilitating dimensionality reduction and clustering analyses. The top 2000 highly variable genes were identified via the `FindVariableFeatures` function with the variance-stabilizing transformation ("vst") method. PCA was performed via the `RunPCA` function on the identified highly variable genes. We used the Harmony package (version 1.2.0) (Korsunsky et al. 2019) to correct batch effects and align cells from different samples. A K-nearest neighbor graph was constructed via the `FindNeighbors` function on the basis of the first 30 Harmony-corrected principal components. The cell clusters were identified via the `FindClusters` function across a range of resolutions (0.1–0.6). Finally, we utilized the `RunUMAP` function to generate uniform manifold approximation and projection (UMAP) plots for data visualization.

Cell type annotation and proportion analysis

Cell type annotation was performed to identify and classify the various cell populations within the scRNA-seq data. Initially, marker genes for each cell population were calculated via the `FindAllMarkers` function in Seurat. Following the identification of marker genes, preliminary cell type annotation was conducted via the SingleR package (V. 2.4.1) (Aran et al. 2019). To ensure accurate and comprehensive cell type annotation, the initial annotations were refined by cross-referencing the identified marker genes with annotations available in the CellMarker 2.0 database (Hu et al. 2023). After the cell type annotations were finalized, the proportions of each cell type within each sample were calculated via the `dplyr` package (V. 1.1.4). To visualize the distribution and proportion of different cell types, stacked bar plots were generated via the `ggplot2` package (V. 3.4.4).

DEG analysis and pathway enrichment analysis

To identify DEGs under H1N1 infection, we utilized the Seurat package's FindMarkers function. This function was employed to perform differential gene expression analysis on the scRNA-seq data. To visualize the DEGs, we used the scRNAtoolVis package (V. 0.0.7) (<https://github.com/junjunlab/scRNAtoolVis>) to generate volcano plots. Additionally, violin plots of DEGs were created via the ggpubr package (V. 0.6.0), with statistical significance assessed via Student's *t* tests. The significance levels were denoted as follows: $P < 0.05$ (*), $P < 0.01$ (**), $P < 0.001$ (***), and $P < 0.0001$ (****). Genes with an average log₂-fold change (avg_log₂FC) greater than or equal to 1 and a *p* value less than or equal to 0.01 were selected for further analysis. These DEGs were subjected to KEGG pathway analysis and gene ontology biological process (GOBP) annotation via the clusterProfiler (V. 4.10.0) package (Wu et al. 2021; Yu et al. 2012). The enrichment analysis results were visualized via the Goplot package (V. 1.0.2) (Walter et al. 2015) and ggplot2.

Intercellular cross-talk analysis

To analyze intercellular cross-talk, we employed the CellChat package (version 1.6.1) (Jin et al. 2021), which provides a comprehensive framework for investigating intercellular communication from scRNA-seq data. For our analysis, we utilized the "Secreted Signaling" database from CellChatDB.human and CellChatDB.mouse, which focuses on signaling pathways mediated by secreted molecules, a crucial aspect of intercellular interactions within the immune system. Using CellChat, we computed the probabilities of communication between different cell types and identified fundamental signaling interactions during the immune response to infection. The analysis allowed us to map the intricate network of signals exchanged among immune cells, revealing insights into how these interactions are altered upon infection. The results of the intercellular cross-talk analysis were visualized via the built-in functions provided by CellChat, which effectively highlighted the significant signaling pathways and the strength of interactions between cell types.

Transcription factor regulation analysis

For transcription factor regulation analysis, we utilized the pySCENIC (version 0.12.1) workflow (Aibar et al. 2017), a comprehensive tool for inferring gene regulatory networks and identifying active transcription factors from scRNA-seq data. The analysis involved several vital steps to ensure accurate and robust identification of transcription factor activity and its regulatory targets. Initially, we constructed a coexpression network via GRNBoost, which infers regulatory relationships

on the basis of single-cell gene expression matrices. Following network construction, we performed motif enrichment and target gene prediction via RcisTarget. This step involves scanning the regulatory regions of coexpressed genes to identify known transcription factor binding motifs, thereby predicting which transcription factors are likely to regulate these genes. To quantify the activity of the identified regulons (transcription factors and their target genes), we employed AUCell, which evaluates the enrichment of regulon target genes within each single-cell expression profile. Subsequent visualization of the results was performed in R. The transcription factor regulatory networks were visualized via the igraph package (version 1.6.0), which enabled the creation of detailed network diagrams illustrating the interactions between transcription factors and their target genes.

Abbreviations

IAV	Influenza A virus
PBMCs	Peripheral blood mononuclear cells
WHO	World Health Organization
ISGs	Interferon-stimulated genes
scRNA-seq	Single-cell RNA sequencing
HC	Healthy control
IA	Human IAV infection
mHC	Mouse Healthy control
mIA	Mouse IAV infection
DEGs	Differentially expressed genes
PCA	Principal component analysis
UMAP	Uniform manifold approximation and projection

Supplementary Information

The online version contains supplementary material available at <https://doi.org/10.1186/s44149-024-00146-7>.

Additional file 1: Supplementary Fig. 1 Sample integration, cell type annotation, and IAV infection status. (A) Cell clustering plots of human samples before and after batch correction. (B) Cell clustering plots of mouse samples before and after batch correction. (C) Heatmap of the top 5 genes for different cell types in human PBMCs. (D) Heatmap of the top 5 genes for different cell types in mouse lungs. (E) Stacked bar plot of the proportion of infected and bystander cells for each cell type in the lungs of H1N1-infected mice. (F) Violin plot of H1N1 gene expression in infected cells from mouse lungs. mHC: Mouse healthy control; mIA: Mouse IAV infection.

Additional file 2: Supplementary Fig. 2 DEGs in bystander immune cells. (A) Number of DEGs in bystander immune cells from H1N1-infected humans and mice. (B) The number of common DEGs in bystander immune cells between humans and mice. (C) Violin plots of the differential expression of vital functional genes in bystander T cells from H1N1-infected and uninfected individuals. (D) Violin plots of the differential expression of crucial functional genes in bystander T cells from H1N1-infected and uninfected mice. HC: Human healthy control, IA: Human IAV infection, mHC: Mouse healthy control, mIA: Mouse IAV infection.

Additional file 3: Supplementary Fig. 3 Analysis of signaling pathways and ligand–receptor pairs involved in the cross-talk of bystander immune cells. (A) Bar plot for the contributions of CCL pathway ligand–receptor pairs to the cross-talk among bystander immune cells of H1N1-infected and uninfected groups from humans and mice. (B) Network diagrams of cross-talk between bystander immune cells from humans and mice on the basis of the *CCL5-CCR1* pair and *Ccl6-Ccr2* pair. (C) Crosstalk heatmap of the TGF- β signaling pathway in bystander immune cells from humans and mice.

(D) Bar plot of the contributions of ligand–receptor pairs from the TGF- β pathway to cross-talk between bystander immune cells from humans and mice. (E) Network diagrams of the cross-talk between bystander immune cells from humans and mice via the *TGFB1*-(*TGFB1*+*TGFB2*) pair and the *Tgfb1*-(*Tgfb1*+*Tgfb2*) pair. HC: Human healthy control, IA: Human IAV infection, mHC: Mouse healthy control, mA: Mouse IAV infection.

Additional file 4: Supplementary Table 1. Differentially expressed genes and enrichment analysis results of bystander immune cells in human PBMCs and mouse lung tissues following H1N1 infection.

Acknowledgements

We thank all the data contributors, especially Yin Zhang and Andrew K. Beppu, for generating single-cell transcriptomic sequencing data related to human and mouse IAV and sharing these datasets through the GEO database (GSE243629, GSE184384).

Authors' contributions

GC, JZ, BY, and JD: Project administration, supervision, writing, review and editing; YC: Data collection, bioinformatics analysis, and writing original draft; HC: Data collection and bioinformatics analysis; QZ: Writing, review and editing. All the authors have read and agreed with the final version of the manuscript.

Funding

This work was supported by the National Natural Science Foundation of China (Grant No. 32330104).

Data availability

The relevant data and material in this article are available and can be requested from the corresponding authors.

Declarations

Ethics approval and consent to participate

Not applicable.

Consent for publication

Not applicable.

Competing interests

The authors declare that they have no competing interests. Author Gang Cao was not involved in the journal's review or decisions related to this manuscript.

Author details

¹National Key Laboratory of Agricultural Microbiology, Huazhong Agricultural University, Wuhan 430070, China. ²College of Life Science and Technology, Huazhong Agricultural University, Wuhan 430070, China. ³College of Veterinary Medicine, Huazhong Agricultural University, Wuhan 430070, China. ⁴College of Informatics, Huazhong Agricultural University, Wuhan 430070, China. ⁵Faculty of Life and Health Sciences, Shenzhen Institute of Advanced Technology, Chinese Academy of Sciences, Shenzhen 518107, China.

Received: 23 July 2024 Accepted: 16 October 2024

Published online: 31 October 2024

References

- Aibar, S., C.B. Gonzalez-Blas, T. Moerman, V.A. Huynh-Thu, H. Imrichova, G. Huiselmans, F. Rambow, J.C. Marine, P. Geurts, J. Aerts, et al. 2017. SCENIC: Single-cell regulatory network inference and clustering. *Nature Methods* 14 (11): 1083–1086. <https://doi.org/10.1038/nmeth.4463>.
- Aran, D., A.P. Looney, L. Liu, E. Wu, V. Fong, A. Hsu, S. Chak, R.P. Naikawadi, P.J. Wolters, A.R. Abate, A.J. Butte, and M. Bhattacharya. 2019. Reference-based analysis of lung single-cell sequencing reveals a transitional profibrotic macrophage. *Nature Immunology* 20 (2): 163–172. <https://doi.org/10.1038/s41590-018-0276-y>.
- Beppu, A.K., J. Zhao, C. Yao, G. Carraro, E. Israely, A.L. Coelho, K. Drake, C.M. Hogaboam, W.C. Parks, J.K. Kolls, and B.R. Stripp. 2023. Epithelial plasticity and innate immune activation promote lung tissue remodeling following respiratory viral infection. *Nat Commun* 14 (1): 5814. <https://doi.org/10.1038/s41467-023-41387-3>.
- Bohlen, J., Q. Zhou, Q. Philippot, M. Ogishi, D. Rinchai, T. Nieminen, S. Seyedpour, N. Parvaneh, N. Rezaei, N. Yazdanpanah, et al. 2023. Human MCTS1-dependent translation of JAK2 is essential for IFN-gamma immunity to mycobacteria. *Cell* 186 (23): 5114–5134 e5127. <https://doi.org/10.1016/j.cell.2023.09.024>.
- Bonjardim, C.A., P.C. Ferreira, and E.G. Kroon. 2009. Interferons: Signaling, antiviral and viral evasion. *Immunology Letters* 122 (1): 1–11. <https://doi.org/10.1016/j.imlet.2008.11.002>.
- Boyd, D.F., E.K. Allen, A.G. Randolph, X.J. Guo, Y. Weng, C.J. Sanders, R. Bajracharya, N.K. Lee, C.S. Guy, P. Vogel, et al. 2020. Exuberant fibroblast activity compromises lung function via ADAMTS4. *Nature* 587 (7834): 466–471. <https://doi.org/10.1038/s41586-020-2877-5>.
- Ciancanelli, M.J., S.X. Huang, P. Luthra, H. Garner, Y. Itan, S. Volpi, F.G. Lafaille, C. Trouillet, M. Schmolke, R.A. Albrecht, et al. 2015. Infectious disease. Life-threatening influenza and impaired interferon amplification in human IRF7 deficiency. *Science* 348 (6233): 448–453. <https://doi.org/10.1126/science.12578>.
- Crouse, J., U. Kalinke, and A. Oxenius. 2015. Regulation of antiviral T-cell responses by type I interferons. *Nature Reviews Immunology* 15 (4): 231–242. <https://doi.org/10.1038/nri3806>.
- Dai, M., S. Zhu, Z. An, B. You, Z. Li, Y. Yao, V. Nair, and M. Liao. 2023. Dissection of key factors correlating with H5N1 avian influenza virus driven inflammatory lung injury of chicken identified by single-cell analysis. *PLoS Pathogens* 19 (10): e1011685. <https://doi.org/10.1371/journal.ppat.1011685>.
- Deshmane, S.L., S. Kremlev, S. Amini, and B.E. Sawaya. 2009. Monocyte chemoattractant protein-1 (MCP-1): An overview. *Journal of Interferon and Cytokine Research* 29 (6): 313–326. <https://doi.org/10.1089/jir.2008.0027>.
- Gordon, S., and A. Pluddemann. 2018. Macrophage clearance of apoptotic cells: A critical assessment. *Frontiers in Immunology* 9:127. <https://doi.org/10.3389/fimmu.2018.00127>.
- Gostic, K.M., R. Bridge, S. Brady, C. Viboud, M. Worobey, and J.O. Lloyd-Smith. 2019. Childhood immune imprinting to influenza A shapes birth year-specific risk during seasonal H1N1 and H3N2 epidemics. *PLoS Pathogens* 15 (12): e1008109. <https://doi.org/10.1371/journal.ppat.1008109>.
- Hage, A., P. Bharaj, S. van Tol, M.I. Giraldo, M. Gonzalez-Orozco, K.M. Valerdi, A.N. Warren, L. Aguilera-Aguirre, X. Xie, S.G. Widen, et al. 2022. The RNA helicase DHX16 recognizes specific viral RNA to trigger RIG-I-dependent innate antiviral immunity. *Cell Reports* 38 (10): 110434. <https://doi.org/10.1016/j.celrep.2022.110434>.
- Hao, Y., T. Stuart, M.H. Kowalski, S. Choudhary, P. Hoffman, A. Hartman, A. Srivastava, G. Molla, S. Madad, C. Fernandez-Granda, et al. 2024. Dictionary learning for integrative, multimodal and scalable single-cell analysis. *Nature Biotechnology* 42 (2): 293–304. <https://doi.org/10.1038/s41587-023-01767-y>.
- Hemann, E.A., R. Green, J.B. Turnbull, R.A. Langlois, R. Savan, and M. Gale Jr. 2019. Interferon-lambda modulates dendritic cells to facilitate T-cell immunity during infection with influenza A virus. *Nature Immunology* 20 (8): 1035–1045. <https://doi.org/10.1038/s41590-019-0408-z>.
- Hu, C., T. Li, Y. Xu, X. Zhang, F. Li, J. Bai, J. Chen, W. Jiang, K. Yang, Q. Ou, X. Li, P. Wang, and Y. Zhang. 2023. Cell Marker 2.0: an updated database of manually curated cell markers in human/mouse and web tools based on scRNA-seq data. *Nucleic Acids Res* 51 (D1): D870–D876. <https://doi.org/10.1093/nar/gkac947>.
- Ivashkiv, L.B., and L.T. Donlin. 2014. Regulation of type I interferon responses. *Nature Reviews Immunology* 14 (1): 36–49. <https://doi.org/10.1038/nri3581>.
- Iwasaki, A., and P.S. Pillai. 2014. Innate immunity to influenza virus infection. *Nature Reviews Immunology* 14 (5): 315–328. <https://doi.org/10.1038/nri3665>.
- Jin, S., C.F. Guerrero-Juarez, L. Zhang, I. Chang, R. Ramos, C.H. Kuan, P. Myung, M.V. Pliusk, and Q. Nie. 2021. Inference and analysis of cell-cell communication using Cell Chat. *Nature Communications* 12 (1): 1088. <https://doi.org/10.1038/s41467-021-21246-9>.
- Kasuga, Y., B. Zhu, K.J. Jang, and J.S. Yoo. 2021. Innate immune sensing of coronavirus and viral evasion strategies. *Experimental & Molecular Medicine* 53 (5): 723–736. <https://doi.org/10.1038/s12276-021-00602-1>.
- Kim, S.B., J.Y. Choi, E. Uyangaa, A.M. Patil, F.M. Hossain, J. Hur, S.Y. Park, J.H. Lee, K. Kim, and S.K. Eo. 2016. Blockage of indoleamine 2,3-dioxygenase

- regulates Japanese encephalitis via enhancement of type I/II IFN innate and adaptive T-cell responses. *Journal of Neuroinflammation* 13 (1): 79. <https://doi.org/10.1186/s12974-016-0551-5>.
- Korsunsky, I., N. Millard, J. Fan, K. Slowikowski, F. Zhang, K. Wei, Y. Baglaenko, M. Brenner, P.R. Loh, and S. Raychaudhuri. 2019. Fast, sensitive and accurate integration of single-cell data with Harmony. *Nature Methods* 16 (12): 1289–1296. <https://doi.org/10.1038/s41592-019-0619-0>.
- Krammer, F., and P. Palese. 2015. Advances in the development of influenza virus vaccines. *Nature Reviews. Drug Discovery* 14 (3): 167–182. <https://doi.org/10.1038/nrd4529>.
- Lazear, H.M., J.W. Schoggins, and M.S. Diamond. 2019. Shared and distinct functions of type I and type III interferons. *Immunity* 50 (4): 907–923. <https://doi.org/10.1016/j.immuni.2019.03.025>.
- Li, X., Z. Dong, J. Li, C. Dou, D. Tian, Z. Ma, W. Liu, G.F. Gao, and Y. Bi. 2024. Genetic characteristics of H1N1 influenza virus outbreak in China in early 2023. *Viral Sin* 39 (3): 520–523. <https://doi.org/10.1016/j.virs.2024.05.003>.
- Liu, S., Y. Liao, B. Chen, Y. Chen, Z. Yu, H. Wei, L. Zhang, S. Huang, P.B. Rothman, G.F. Gao, and J.L. Chen. 2021. Critical role of Syk-dependent STAT1 activation in innate antiviral immunity. *Cell Reports* 34 (3): 108627. <https://doi.org/10.1016/j.celrep.2020.108627>.
- Mao, H., Y. Sun, Y. Chen, X. Lou, Z. Yu, X. Wang, Z. Ding, W. Cheng, D. Zhang, Y. Zhang, and J. Jiang. 2020. Cocirculation of influenza A(H1N1), A(H3N2), B(Yamagata) and B(Victoria) during the 2017–2018 influenza season in Zhejiang Province, China. *Epidemiol Infect* 148: e296. <https://doi.org/10.1017/S0950268820000412>.
- Medaglia, C., I. Kolpakov, A.C. Zwygart, Y. Zhu, S. Constant, S. Huang, V. Cagno, E.T. Dermitzakis, F. Stellacci, I. Xenarios, et al. 2022. An anti-influenza combined therapy assessed by single cell RNA-sequencing. *Commun Biol* 5 (1): 1075. <https://doi.org/10.1038/s42003-022-04013-4>.
- Music, N., A.J. Reber, J.H. Kim, and I.A. York. 2016. Peripheral leukocyte migration in ferrets in response to infection with seasonal influenza virus. *PLoS ONE* 11 (6): e0157903. <https://doi.org/10.1371/journal.pone.0157903>.
- O'Neill, M.B., H. Quach, J. Pothlichet, Y. Aquino, A. Bisiaux, N. Zidane, M. Deschamps, V. Libri, M. Hasan, S.Y. Zhang, et al. 2021. Single-cell and bulk RNA-sequencing reveal differences in monocyte susceptibility to influenza A virus infection between Africans and Europeans. *Frontiers in Immunology* 12: 768189. <https://doi.org/10.3389/fimmu.2021.768189>.
- Park, J. E., Botting, R. A., Dominguez Conde, C., Popescu, D. M., Lavaert, M., Kunz, D. J., Goh, I., Stephenson, E., Ragazzini, R., Tuck, E., et al. 2020. A cell atlas of human thymic development defines T-cell repertoire formation. *Science*, 367(6480). <https://doi.org/10.1126/science.aay3224>
- Perng, Y.C., and D.J. Lenschow. 2018. ISG15 in antiviral immunity and beyond. *Nature Reviews Microbiology* 16 (7): 423–439. <https://doi.org/10.1038/s41579-018-0020-5>.
- Pizzolla, A., and L.M. Wakim. 2019. Memory T-cell dynamics in the lung during influenza virus infection. *The Journal of Immunology* 202 (2): 374–381. <https://doi.org/10.4049/jimmunol.1800979>.
- Ren, X., D. Wang, G. Zhang, T. Zhou, Z. Wei, Y. Yang, Y. Zheng, X. Lei, W. Tao, A. Wang, M. Li, R.A. Flavell, and S. Zhu. 2023. Nucleic DHX9 cooperates with STAT1 to transcribe interferon-stimulated genes. *Sci Adv* 9 (5): eadd5005. <https://doi.org/10.1126/sciadv.add5005>.
- Russell, C.D., S.A. Unger, M. Walton, and J. Schwarze. 2017. The Human immune response to respiratory syncytial virus infection. *Clinical Microbiology Reviews* 30 (2): 481–502. <https://doi.org/10.1128/CMR.00090-16>.
- Schoggins, J.W. 2014. Interferon-stimulated genes: Roles in viral pathogenesis. *Current Opinion in Virology* 6: 40–46. <https://doi.org/10.1016/j.coviro.2014.03.006>.
- Schoggins, J.W., and C.M. Rice. 2011. Interferon-stimulated genes and their antiviral effector functions. *Current Opinion in Virology* 1 (6): 519–525. <https://doi.org/10.1016/j.coviro.2011.10.008>.
- Stadler, D., M. Kachele, A.N. Jones, J. Hess, C. Urban, J. Schneider, Y. Xia, A. Oswald, F. Nebioglu, R. Bester, et al. 2021. Interferon-induced degradation of the persistent hepatitis B virus cccDNA form depends on ISG20. *EMBO Rep* 22 (6): e49568. <https://doi.org/10.15252/embr.201949568>.
- Steuerman, Y., M. Cohen, N. Peshes-Yaloz, L. Valadarsky, O. Cohn, E. David, A. Frishberg, L. Mayo, E. Bacharach, I. Amit, and I. Gat-Viks. 2018. Dissection of influenza infection in vivo by single-cell RNA sequencing. *Cell Syst* 6 (6): 679–691 e674. <https://doi.org/10.1016/j.cels.2018.05.008>.
- Sun, J., J.C. Vera, J. Drnevich, Y.T. Lin, R. Ke, and C.B. Brooke. 2020. Single cell heterogeneity in influenza A virus gene expression shapes the innate antiviral response to infection. *PLoS Pathogens* 16 (7): e1008671. <https://doi.org/10.1371/journal.ppat.1008671>.
- Vangeti, S., Falck-Jones, S., Yu, M., Osterberg, B., Liu, S., Asghar, M., Sonden, K., Paterson, C., Whitley, P., Albert, J., Johansson, N., Farnert, A., and Smed-Sorensen, A. 2023. Human influenza virus infection elicits distinct patterns of monocyte and dendritic cell mobilization in blood and the nasopharynx. *Elife*, 12. <https://doi.org/10.7554/eLife.77345>
- Walter, W., F. Sanchez-Cabo, and M. Ricote. 2015. GPlot: An R package for visually combining expression data with functional analysis. *Bioinformatics* 31 (17): 2912–2914. <https://doi.org/10.1093/bioinformatics/btv300>.
- Wang, YX., M. Niklasch, T. Liu, Y. Wang, B. Shi, W. Yuan, T.F. Baumert, Z. Yuan, S. Tong, M. Nassal, and Y.M. Wen. 2020. Interferon-inducible MX2 is a host restriction factor of hepatitis B virus replication. *Journal of Hepatology* 72 (5): 865–876. <https://doi.org/10.1016/j.jhep.2019.12.009>.
- White, M.R., N.M. Nikolaidis, F. McCormack, E.C. Crouch, and K.L. Hartshorn. 2021. Viral evasion of innate immune defense: The case of resistance of pandemic H1N1 influenza A virus to human mannose-binding proteins. *Frontiers in Microbiology* 12: 774711. <https://doi.org/10.3389/fmicb.2021.774711>.
- Wilk, A.J., A. Rustagi, N.Q. Zhao, J. Roque, G.J. Martinez-Colon, J.L. McKechnie, G.T. Ivison, T. Ranganath, R. Vergara, T. Hollis, et al. 2020. A single-cell atlas of the peripheral immune response in patients with severe COVID-19. *Nature Medicine* 26 (7): 1070–1076. <https://doi.org/10.1038/s41591-020-0944-y>.
- Wu, T., E. Hu, S. Xu, M. Chen, P. Guo, Z. Dai, T. Feng, L. Zhou, W. Tang, L. Zhan, X. Fu, S. Liu, X. Bo, and G. Yu. 2021. clusterProfiler 4.0: A universal enrichment tool for interpreting omics data. *Innovation (Camb)* 2 (3): 100141. <https://doi.org/10.1016/j.xinn.2021.100141>.
- Yang, J., Y. Gong, C. Zhang, J. Sun, G. Wong, W. Shi, W. Liu, G.F. Gao, and Y. Bi. 2022. Coexistence and coinfection of influenza A viruses and coronaviruses: Public health challenges. *Innovation (Camb)* 3 (5): 100306. <https://doi.org/10.1016/j.xinn.2022.100306>.
- Yu, G., L.G. Wang, Y. Han, and Q.Y. He. 2012. clusterProfiler: An R package for comparing biological themes among gene clusters. *OMICS: A Journal of Integrative Biology* 16 (5): 284–287. <https://doi.org/10.1089/omi.2011.0118>.
- Zhang, Y., L. Zong, Y. Zheng, Y. Zhang, N. Li, Y. Li, Y. Jin, L. Chen, J. Ouyang, A. Bibi, Y. Huang, and Y. Xu. 2023. A single-cell atlas of the peripheral immune response in patients with influenza A virus infection. *iScience* 26 (12): 108507. <https://doi.org/10.1016/j.isci.2023.108507>.
- Zhao, C., M.N. Collins, T.Y. Hsiang, and R.M. Krug. 2013. Interferon-induced ISG15 pathway: An ongoing virus-host battle. *Trends in Microbiology* 21 (4): 181–186. <https://doi.org/10.1016/j.tim.2013.01.005>.
- Zhao, G., L. Xue, A.I. Weiner, N. Gong, S. Adams-Tzivelekidis, J. Wong, M.E. Gentile, A.N. Nottingham, M.C. Basil, S.M. Lin, et al. 2024. TGF-betaR2 signaling coordinates pulmonary vascular repair after viral injury in mice and human tissue. *Sci Transl Med* 16 (732): eadg6229. <https://doi.org/10.1126/scitranslmed.adg6229>.
- Zhou, H., Y.D. Tang, and C. Zheng. 2022. Revisiting IRF1-mediated antiviral innate immunity. *Cytokine & Growth Factor Reviews* 64: 1–6. <https://doi.org/10.1016/j.cytogfr.2022.01.004>.
- Zhu, Z., R. Mao, B. Liu, H. Liu, Z. Shi, K. Zhang, H. Liu, D. Zhang, J. Liu, Z. Zhao, et al. 2024. Single-cell profiling of African swine fever virus disease in the pig spleen reveals viral and host dynamics. *Proc Natl Acad Sci U S A* 121 (10): e2312150121. <https://doi.org/10.1073/pnas.2312150121>.

Publisher's Note

Springer Nature remains neutral with regard to jurisdictional claims in published maps and institutional affiliations.